Title
SOLID-STATE DEVICES AS DETECTORS OF COHERENT HIGH-ENERGY INTERACTIONS

Authors
Lander, Richard L.
Mehlhop, Werner A.W.
Lubatti, H.J.
et al.

Publication Date
1965-12-30

UCRL-16603

c.2

University of California

Ernest O. Lawrence Radiation Laboratory

SOLID-STATE DEVICES AS DETECTORS
OF COHERENT HIGH-ENERGY INTERACTIONS

Berkeley, California

DISCLAIMER

Nuclear Instruments and Methods

UCRL-16603

UNIVERSITY OF CALIFORNIA

Lawrence Radiation Laboratory
Berkeley, California

AEC Contract No. W-7405-eng-48

SOLID-STATE DEVICES AS DETECTORS OF COHERENT HIGH-ENERGY INTERACTIONS

Richard L. Lander, Werner A. W. Mehlhop
H. J. Lubatti, and Gerald L. Schnurmacher

December 30, 1965

SOLID-STATE DEVICES AS DETECTORS OF COHERENT HIGH-ENERGY INTERACTIONS*

Richard L. Lander and Werner A. W. Mehlhop
University of California, San Diego, California

H. J. Lubatti
University of California, Berkeley, California

Gerald L. Schnurmacher
Lawrence Radiation Laboratory
University of California, Berkeley, California

December 30, 1965

ABSTRACT

We consider the possibility of using a solid-state radiation detector as a target in order that the recoil energy of the struck nucleus, as well as any charged nuclear fragments, may be measured. In this way, one can discriminate against those interactions leading to breakup of the nucleus (noncoherent) and can also measure the momentum transfer to the nucleus with considerably better precision than might otherwise be possible. As a first test of such a detector, we have observed the distribution in energy deposited in a 1-mm-thick lithium-drifted silicon detector when 730-MeV protons are scattered at small angles by nuclei in the detector. When the protons traverse the silicon without interacting, the characteristic Landau energy-loss distribution is observed. When the protons scatter at small angles, their energies and path lengths in the silicon are practically unchanged. The recoil silicon nucleus, however, deposits most of its kinetic energy, T_{Si}. This energy is added to that from the proton, so the

---

*Work sponsored by the U. S. Atomic Energy Commission under contracts W-7405-eng-48 and AT-(11-1)-gen 10, Program Agreement 10.

observed energy distribution in the silicon detector is shifted upwards by T_{Si} when the proton scatters. We have observed this second peak at proton scattering angles of 4.3, 5.4, and 6.3 deg in the laboratory system and confirm the predicted energy shift. The potential applications of this technique are discussed.

1. Introduction

This communication describes a new experimental technique that we believe will be of considerable value in elementary-particle physics research. The device employed is a solid-state particle detector. Such devices have been known to physicists for many years and have been used extensively in low-energy nuclear physics. Their application in high-energy physics has been quite limited, largely because most efforts have been directed toward using them in the same fashion as plastic scintillators, without taking advantage of their unique properties. Our technique employs the device as a target as well as a detector. This means the target particle is a nucleus--Si^{28} for example--rather than a proton, which up to now has been the most popular target for elementary-particle experiments. This popularity stems from the relative simplicity of the proton. However, Si^{28} is an even-even nucleus and has zero spin and isospin, so that it is an even simpler target, provided it retains its identity after the interaction. As has been pointed out by Good and Walker[1] and further discussed by A. Goldhaber and M. Goldhaber[2], such interactions may occur when the momentum transfer to the target nucleus is sufficiently small that the interaction takes place coherently over the whole nucleus. The essential point of our technique is that we can measure the momentum transferred to the target nucleus, and therefore can separate coherent interactions from those leading to nuclear breakup.

As a feasibility test of this technique, we have observed at the Berkeley 184-Inch Cyclotron the nuclear recoils from coherent (elastic) scattering of 730-MeV protons by silicon nuclei at values of momentum transfer to the nucleus of 105, 132, and 152-MeV/c (which correspond to scattering

angles of 4.3, 5.4, and 6.3 deg, respectively). The measured pulse heights observed from the solid-state detector were as expected for recoiling silicon nuclei of these momenta, which we take as demonstrating that the nucleus was not disrupted.

2. Experimental Apparatus and Electronic Logic

The experimental arrangement and the electronic block diagram are shown in Figs. 1 and 2, respectively. Counters S_1 through S_7 were standard scintillation counters, made of plastic scintillator material and coupled to RCA 6810A photomultiplier tubes. The electronic logic was assembled from the "Chronetics" line of fast modular counting electronics. Counter pulses were standardized to 20-nsec width by the use of fast discriminators. This pulse width greatly reduced the problem of timing the counters, although it was still short enough to give a negligible contribution of accidental coincidences (at incident beam levels of 10^4 protons/sec).

Counters S_1 and S_2, in coincidence, defined the incident beam. This beam then struck the solid-state detector SSD (to be discussed in detail below). Elastic scatters from this target (SSD) were selected by counters S_5 and S_6, which consisted of annular scintillators (the ring shape provides an increased solid angle); they were geometrically arranged so as to define a scattering angle of a few degrees (see below for detailed settings) with an angular acceptance range of approximately one degree. Counters S_3, S_4, and S_7 were connected in anticoincidence in order to further assure that only events of the desired kind were accepted. Counters S_3 and S_4 each had a 1-in.-diam hole centered on the incident beam line; thus they required that the scattered particle originate at SSD rather than, say, at S_1 or S_2. Counter S_7 was used to veto the unscattered beam.

An elastic-scattering event, then, was signalled by the electronic logic in the form of a signal $S_1S_2S_5S_6\bar{S}_3\bar{S}_4\bar{S}_7$. Furthermore, one could easily obtain a logical signal signifying a straight-through beam proton via $S_1S_2S_7$. The procedure of the experiment may thus be summarized as follows: after having obtained a logical signal of either of these two kinds, one interrogates the SSD as to the kind of signal resulting from it.

The electrical pulse from the SSD was fed into a preamplifier and from there into a linear amplifier gating and timing system[3]. This kind of transistorized system is by now standard in SSD work.* The preamplifier of the charge-sensitive kind, provides the low impedance necessary to drive a cable[4]. The linear amplifier is capable of conserving the high-energy resolution of the detector, while the rest of the system provides a fast-coincidence signal via the zero-crossing method, has a linear gate to minimize pileup, and has an output stage suitable to drive a conventional pulse-height analyzer.

The interrogation of the SSD was accomplished by gating this system with the output of the electronic logic in fast coincidence and displaying the amplifier output of the SSD on a pulse-height analyzer. For example, the energy loss spectrum of nonscattered beam particles traversing the silicon wafer is shown in Figs. 3(a) and (b). The characteristic Landau shape is apparent[5]. The energy-spectrum scale was calibrated using 390-keV electrons from a Sn^{113} source. The expected peak of this Landau distribution is 415 keV, which is in good agreement with the data.

---

*Units of the Goulding-Landis type are made commercially by Ortec, Oak Ridge, Tennessee, and by Technical Measurements Corporation, Northhaven, Connecticut.

3. Solid-State Detector

The lithium-drifted-silicon type, solid-state device used as the target-detector in the experiment was fabricated at Lawrence Radiation Laboratory (LRL) by the Nuclear Chemistry Instrumentation Group. The fabrication procedure has been described by Lothrop and Smith[6].

The sensitive region of the detector was 1.09 mm thick and 15 mm in diam. A diagram of the detector is shown in Fig. 4. Figure 5 gives a view of both sides of the detector. The left-hand view shows the cathode side of the detector with its large-diameter gold surface. This gold surface constitutues a thin window about 2000 Å thick, through which particles must pass before traversing the lithium-drifted region. The anode, mesa side of the detector shown in the right-hand view has a lithium-diffused layer on the order of 5×10^{-3} cm thick which is similarly covered by a very thin layer of evaporated gold.

The detector holder used is shown in Fig. 6. Because the detector becomes photosensitive when voltage is applied to it, the holder was made light-tight by covering the beam-entrance and exit side with a thin layer of black photographic tape. The beam-entrance side of the SSD was at ground potential, and positive voltage was applied to the beam-exit side via a 0.004-in.-thick, phosphor-bronze cat's whisker soldered to the center conductor of a BNC connector. Besides being used to apply high voltage to the detector, the cat's whisker served the additional function of spring loading the detector wafer, thereby keeping it aligned in its mount. The single BNC connector was used both to apply high voltage to the detector and to receive the output signal. A potential of 120 V was applied to the detector, with a corresponding leakage current of ~5 μA.

Without going into detail, let us mention some of the problems pertaining to leakage current and detector thickness. With any SSD, one needs to apply a voltage sufficient to collect the charges produced by the radiation to be detected. Here, one must compromise between the desired collection and the problem of increased leakage current at higher applied voltages. If the problem of leakage current and the corresponding loss of resolution is serious, one can usually alleviate it by cooling the detectors to -50 to -100°C. Also, the problem of leakage current increases with increasing detector thickness.

We did not survey commercial suppliers of lithium-drifted silicon detectors to determine maximum diameter and detector thickness available; however, at the Lawrence Radiation Laboratory where our detector was made, the maximum thickness of the sensitive region of lithium-drifted silicon detectors is 5 mm. (These detectors are used only in the cooled state. The maximum sensitive-area thickness of room-temperature detectors is 3 mm.) The maximum diameter of the sensitive region can be made approximately 16 mm with an overall diameter of approximately 18 to 24 mm[7]. Maximum size is dependent on the availability of high-quality, floating-zone, P-type silicon from which the wafers are cut.

Table 1 shows the isotopic composition, spin, parity, and isotopic spin of naturally occurring silicon as used in the detector. As can be seen from the table, a small amount of Si^{29} is present which has different spin-parity and isotopic spin than Si^{28} of which the detector is predominantly composed.

Detectors available from commercial suppliers vary somewhat in cost, but generally the cost is no more than that of 2 or 3 photomultiplier tubes of the variety in common usage in scintillator experiments.

The effects of radiation damage to lithium-drifted silicon detectors is somewhat complex and dependent on many parameters, primary of which is the type of particle causing the damage. Goulding in a recent paper discussed this topic in some detail[8]. In the experiment described herein, there were no effects of radiation damage.

The energy resolution of our detection system was approximately 60 keV at room temperature, entirely sufficient for our experiment. Therefore, we did not cool our detector in order to improve the resolution. A comparison of typical energy-resolution values of various types of counters versus solid-state detectors is given in Table 2.

4. Results

The essential data of this experiment are the pulse-height spectra observed from the SSD target when 730-MeV protons were scattered by the silicon nuclei in it. Four such spectra were obtained, corresponding to scattering angles of 0 (i.e., no scattering at all other than ~0.03 deg multiple Coulomb), 4.3, 5.4, and 6.3 deg.

Consider first the zero-degree "scattering". As mentioned in Section 2, when the trigger logic is set for 0 deg ($S_1 S_2 S_7$), the pulse-height spectrum represents the ionization-energy loss distribution of unscattered protons passing through the SSD. The observed spectrum is shown in Fig. 3. The energy scale was calibrated using 390-keV electrons from a windowless Sn^{113} source. These electrons gave a distribution with a full width of 60 keV. Since the natural width of the 390-keV electron distribution is much less than 60 keV, this value was taken as the resolution of the detector system. The theoretically expected distribution, known as the Landau distribution, was taken from tables by Seltzer and Berger[9], and is shown as the

solid curve of Fig. 3(b). The curve includes an estimate of the effect of the 60-keV resolution of the detector system. The most probable energy loss observed in this experiment (425 ± 10 keV) agrees quite well with the theoretical value (415 keV), but the observed full width at half maximum is about 20% larger than theory predicts.

When we trigger on scattered protons ($S_1S_2S_5S_6\bar{S}_3\bar{S}_4\bar{S}_7$ plus the SSD in coincidence) we expect the pulse-height distribution to exhibit this same Landau shape, since the protons pass through the Si with essentially the same path length and velocity. In addition, the recoiling silicon nucleus loses most of its energy by ionization, so that the Landau distribution is shifted to higher values by an amount equal to the recoil energy deposited in the SSD. However, this shifted Landau distribution will be broadened by the finite angular acceptance of the system. If the trigger is imperfect, such that the signal from straight-through (unscattered) protons reaches the pulse-height analyzer in addition to the pulses from scattering events, then two peaks will be observed in the spectrum. This was the case in our experiment.

The separation of the two peaks represents the energy deposited by the recoiling nucleus. The pulse-height spectra observed for the three scattering angles investigated are shown in Fig. 7. In each case, the two peaks are evident. The lower-energy peak remains at ~ 415 keV as the scattering angles change, while the energy of the second peak decreases with decreasing scattering angle. The solid curve drawn through the data points of the first peak was obtained by drawing a visual-best-fit curve through the data of Fig. 3(b). If all of the energy from the recoil Si nucleus goes into the creation of hole-electron pairs, then the observed shift will correspond to the full energy of the recoil nucleus as

calculated from the momentum and scattering angle of the proton. However, it is known that part of the energy is lost to atomic processes. The three scattering angles used in the experiment and the observed and expected energy shifts are listed in Table 3. The last column in Table 3 shows the ratio of the observed to the expected shift. The fraction of the recoil energy that is lost in the creation of hole-electron pairs has been calculated by Lindhard[10] and experimentally tested by Sattler[11]. Figure 8 shows the theoretical expectation (solid curve) and the experimental data for Si recoils in a Si lattice. Our data(solid circles) as well as Sattler's are seen to be in fair agreement with the theoretical prediction.

5. Discussion

The above results clearly indicate that it is feasible to use the SSD as a detector-target in combination with conventional spark-chamber and counter techniques. Experimentally this affords the distinct advantages of (1) accurately measuring momentum transfers of a few tens of kilovolts or more by recording the pulse from the detector target and (2) using this pulse in a fast-logic system to trigger spark chambers or counters. Nuclear breakup can be detected on the basis of the pulse height, since lighter fragments have greater energy for a given momentum than has silicon.

In addition, the silicon detector target offers a $J = 0$ and $I = 0$ target, which has the advantage of greatly simplifying the analysis of multiparticle final states, provided the target remains in its ground state, as it does for coherent production. Such production also acts as a "cross-section amplifier," because the coherency requirement provides a factor of A^2 times the free-nucleon cross section at a given value of the momentum transfer. Of course, the coherency requirement also limits the momentum

transfer to values of ~ 100 MeV/c, but since most of the physics done today with proton targets involves peripheral interactions, this requirement should not severely limit the physics that can be done with this technique.

A few experiments that come to mind are listed below:

(1) Production experiments in general, of the type X + Nucleus → Y + Nucleus.

Here Y may be a multiparticle state as for example, the experiment of Allard et al. which studied the high-energy production of multipion final states on nuclei by 16-GeV/c pions in a heavy-liquid bubble chamber[12]. The essential idea here is that the SSD would contain the spin-zero target and provide a measurement of the momentum of the recoiling target. This measurement could then be used to trigger thin-plate spark chambers, which would provide an accurate momentum measurement of the final-state bosons. Knowledge of the momentum of the recoil nucleus, which is not possible in the heavy-liquid bubble-chamber experiment, provides an additional constraint for the kinematic fitting. The invariant mass, M_y of the multiboson final state is limited by kinematics. For small momentum transfers, the minimum momentum transfer, q, to the nucleus is given by $q = (M_y^2 - M_x^2)/2P_0$, where P_0 and M_x are the momentum and mass respectively of the incident particle. Since coherency requires that q be ~ 100 MeV/c, we see that mass values up to ~ 2.5 GeV can be produced by the BNL or CERN accelerators, and mass values up to ~ 6.5 GeV by a 200-GeV accelerator. Of course, final states other than bosons may be produced in this way also, and neutral incident particles may be used.

(2) Measurement of the ratio of the real to imaginary part of the forward proton-proton scattering amplitude by observing Coulomb-interference effects in small-angle p-Si elastic scattering.

Using Si as a target removes the complication of the spin-flip term in the strong-interaction amplitude which beclouds the experiments that have been performed on hydrogen; observation of the pulse of the recoiling Si atom in the SSD provides a trigger for selecting small-angle scattering. Of course, one must be able to relate the measured Si cross section to the proton-proton scattering amplitudes. Attempts to do this are currently under way[13].

(3) Regeneration of K_1^0 mesons from a K_2^0 beam incident upon a regenerator.

This can occur in three ways--on a single nucleon, coherently over a nucleus, or coherently over the whole regenerating substance[14]. These three phenomena have different momentum-transfer distributions. The pulse height in a silicon regenerating medium may facilitate separation or selection of the different interactions. Additionally, elastic scattering of K^+ and K^- by Si would be used to obtain precisely the forward-scattering amplitudes for K^0 and $\bar{K}^0$, which are needed for calculating the expected regeneration rates.[2]

(4) Deuteron stripping by nuclei.

There are two as yet unobserved but theoretically expected forms of stripping of incident deuterons by target nuclei--photodissociation of the deuteron in the Coulomb field of the nucleus, and diffraction dissociation of the deuteron[15]. The usual nuclear stripping of high-energy deuterons should lead to breakup of the nucleus. The use of a SSD as a target would enable one to discriminate against this form of stripping and thus facilitate the search for other kinds of stripping.

(5) Detection of the double-charge-exchange process.

Parsons, Trefil, and Drell suggest using the reaction $\pi^{\pm} + A(Z) \rightarrow \pi^{\pm} + A(Z \pm 2)$ to probe nuclear structure[16]. The reaction $\pi^- + Si^{28} \rightarrow \pi^+ + Mg^{28}$ can be studied with the solid-state detector-target, and the pulse height may be used to reduce unwanted background from nuclear breakup.

Acknowledgments

It is a pleasure to acknowledge the assistance of J. Vale and the crew of the 184-Inch Cyclotron. We also would like to thank F. Goulding, D. Landis, and R. Lothrop of the Nuclear Instrumentation Group for providing us with a solid-state detector and a Goulding-Landis electronic system. We have benefited from several discussions with C. Wiegand and H. Steiner. Two of us (RLL and HJL) would like to thank the first International Pacific Summer School at the University of Hawaii, where part of this paper was written, for its hospitality. The interest and support of O. Piccioni is gratefully acknowledged.

References

1) M. Good and W. Walker, Phys. Rev. 120 (1960) 1857.

2) A. Goldhaber and M. Goldhaber, "Coherent High Energy Reactions with Nuclei" (to be published in V. F. Weisskopf Festschrift).

3) F. S. Goulding and D. Landis, NAS-NRC Publication 1184, 1964, p. 124.

4) F. S. Goulding and D. Landis, NAS-NRC Publication 1184, 1964, p. 61.

5) The energy deposited by high-energy charged particles traversing a thin target is distributed asymmetrically about a most probable value. The distribution is essentially Gaussian on the lower-energy side, but has a "tail" on the higher energy side and is known as the Landau distribution. See, for example, E. Segrè, Nuclear Physics (W. A. Benjamin, Inc., New York, 1964), p. 44; or B. Rossi, High Energy Particles, (Prentice-Hall, 1956), p. 34.

6) R. P. Lothrop and H. E. Smith, UCRL-16190, June 1965, unpublished.

7) R. P. Lothrop, Lawrence Radiation Laboratory, private communication.

8) Fred S. Goulding, UCRL-16231, July 1965, unpublished.

9) S. Seltzer and M. Berger, NAS-NRC Publication 1133, 1964, p. 187.

10) J. Lindhard, V. Nielsen, M. Scharff, and P. V. Thomsen, Kgl. Danske Videnskab. Selskab, Mat. Fys. Medd. 33 (1963) No. 10.

11) A. R. Sattler, Phys. Rev. 138 (1965) A1815.

12) J. F. Allard et al., Phys. Letters 12 (1964) 143.

13) A. Goldhaber, Physics Department, University of California, Berkeley, private communication.

14) R. H. Good, R. P. Matson, F. Muller, O. Piccioni, W. M. Powell, H. S. White, W. B. Fowler, and R. W. Birge, Phys. Rev. 124 (1961) 1223.

15) R. J. Glauber, Phys. Rev. 99 (1955) 1515.

16) R. G. Parsons, J. S. Trefuk, and S. D. Drell, Phys. Rev. 138 (1965) B847, and references therein.

Table 1. Characteristics of the silicon used in the solid-state detector.*

Isotope	Excitation energy (MeV)	Spin and parity†		Isospin†		Natural abundance
		J_0^P	J_1^P	I_0	I_1	(%)
Si^{28}	1.78	0^+	2^+	0	0(?)	92.2
Si^{29}	1.28	$1/2^+$	$3/2^+$	1/2(?)	1/2(?)	4.7
Si^{30}	2.23	0^+	0^+	0	0(?)	3.1

*Data are from Endt and Van Der Lenn, Nucl. Phys. 34, 1 (1962).

†Subscripts 0 and 1 refer to ground state and first excited state, respectively.

Table 2. Typical energy-resolution values (full width at half maximum) of various types of detectors.*

Type of detector	Energy resolution (keV)			
	E=100 keV(β)	1 MeV(α)	10 MeV(α)	100 MeV(α)
Gas	30	30	30	
Scintillation	15	50	200	1000
Semiconductor (25°C)	8	10	12	50
Semiconductor (77°C)	3	7	?	?

*Data are from Fred S. Goulding, A Survey of the Applications and Limitations of Various Types of Detectors in Radiation Measurement, UCRL-11302, February 1965.

Table 3. Comparison of observed and expected recoil energies. ΔE transferred is $(P_0 \sin\theta)^2/2M$, where P_0 is the incident momentum, θ is the laboratory scattering angle, and M is the proton mass.

Scattering angle (deg)	ΔE observed (keV)	ΔE transferred (keV)	ΔE obs./ΔE trans.
6.5 ± 1.0	350 ± 24	446	0.78 ± 0.05
5.4 ± 0.9	272 ± 15	330	0.82 ± 0.05
4.3 ± 0.7	140 ± 18	200	0.70 ± 0.09

Figure Legends

Fig. 1. Counter geometry. S_1 through S_7 are plastic scintillators. SSD is the solid-state detector. See text for details.

Fig. 2. Block diagram of electronics.

Fig. 3. (a) Pulse-height distribution from solid-state detector when 730-MeV protons pass through without scattering.
(b) Same data as 3(a) on a semilog plot. The solid curve is the theoretically expected distribution of Ref. 10.

Fig. 4. Cross section of lithium-drifted silicon detector.

Fig. 5. Photograph of detector used in this experiment showing both front and back surfaces.

Fig. 6. Solid-state detector and holder.

Fig. 7. Pulse-height distributions from solid-state detector when protons are scattered from detector at angles (a) 6.5, (b) 5.4, and (c) 4.3 deg. (d, e, f) Same data as a, b, and c, respectively, on a semilog plot. The solid curve through the second peak in each frame is a visual fit to the data. The solid curve through the first peak is a visual fit to the data of Fig. 3b. The dotted curve is the difference of the two solid curves.

Fig. 8. Ionization by a silicon recoil atom in silicon relative to an electron of the same energy. The open data points are from Sattler, and the solid curve is the theoretically expected distribution (see Ref. 12). The three solid circles are from this experiment.

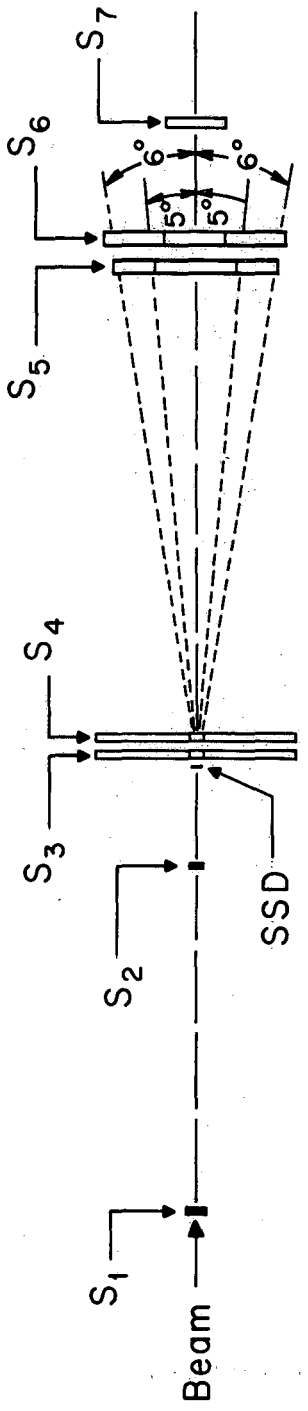

Fig. 1

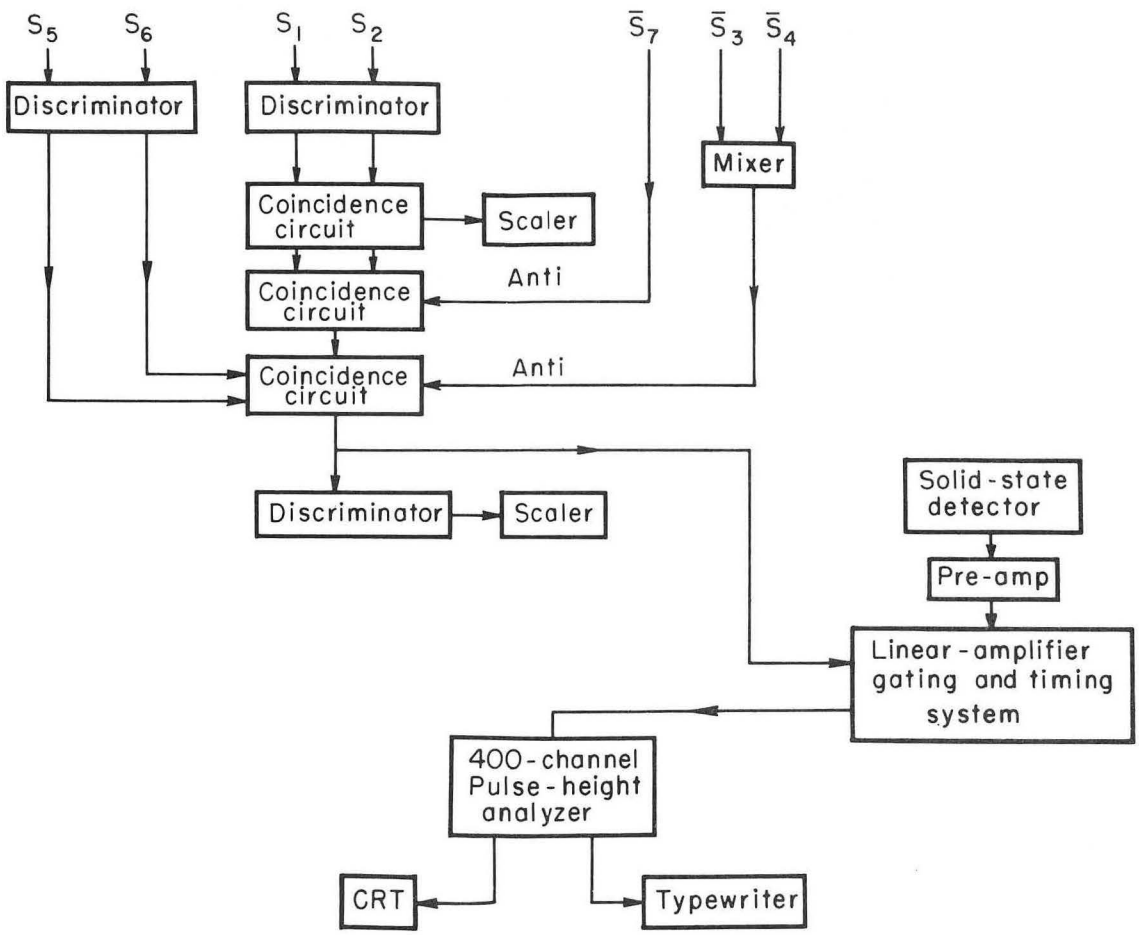

MUB-9233

Fig. 2

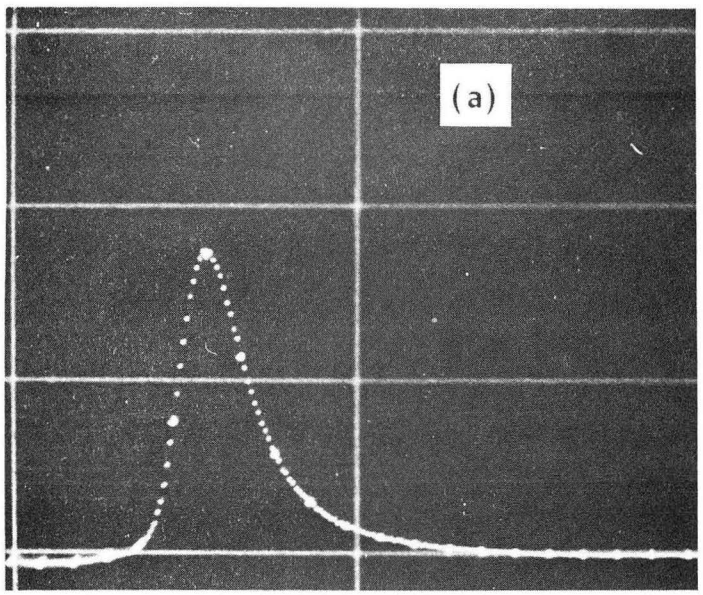
(a)

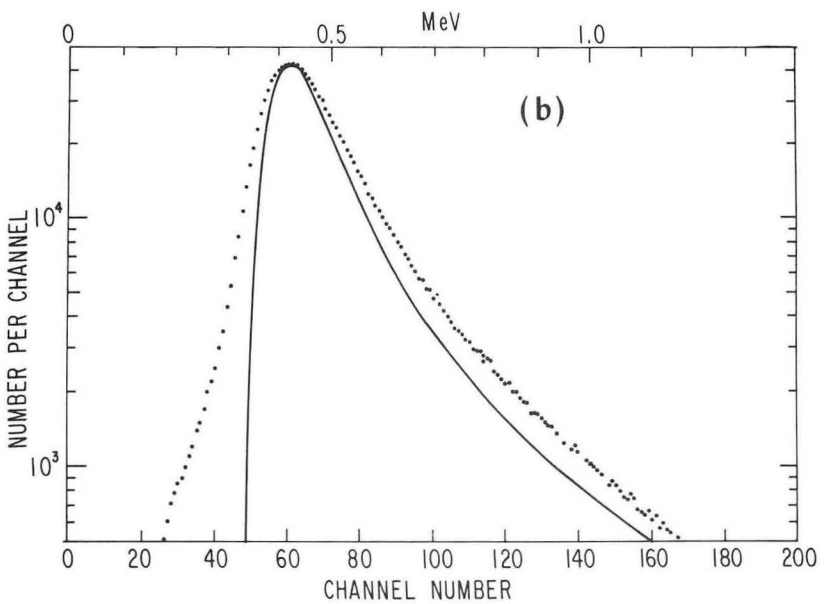
0
0.5
MeV
1.0
(b)
NUMBER PER CHANNEL
10^4
10^3
0
20
40
60
80
100
120
140
160
180
200
CHANNEL NUMBER

ZN-5363

Fig. 3

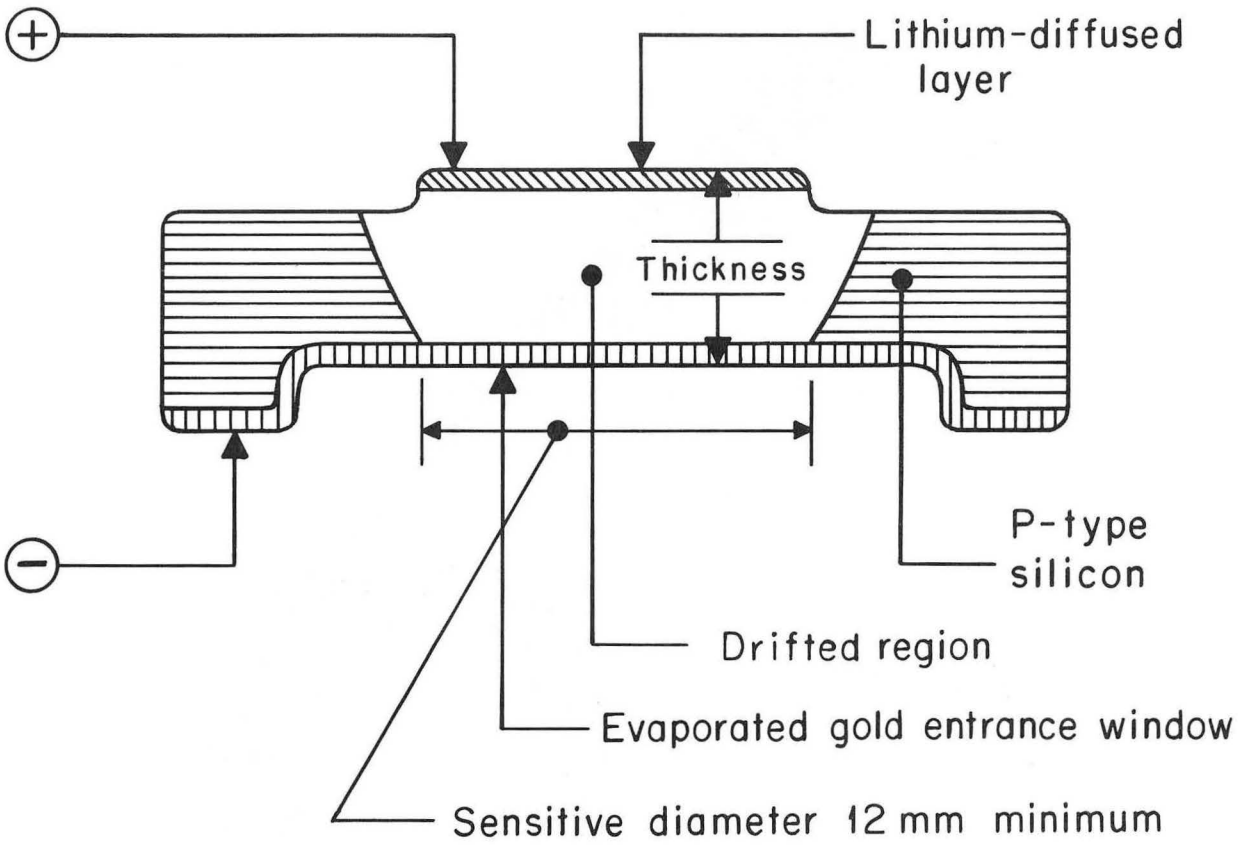
Lithium-diffused layer
Thickness
P-type silicon
Drifted region
Evaporated gold entrance window
Sensitive diameter 12 mm minimum
MUB-4762

Fig. 4

ZN-5365

Fig. 5

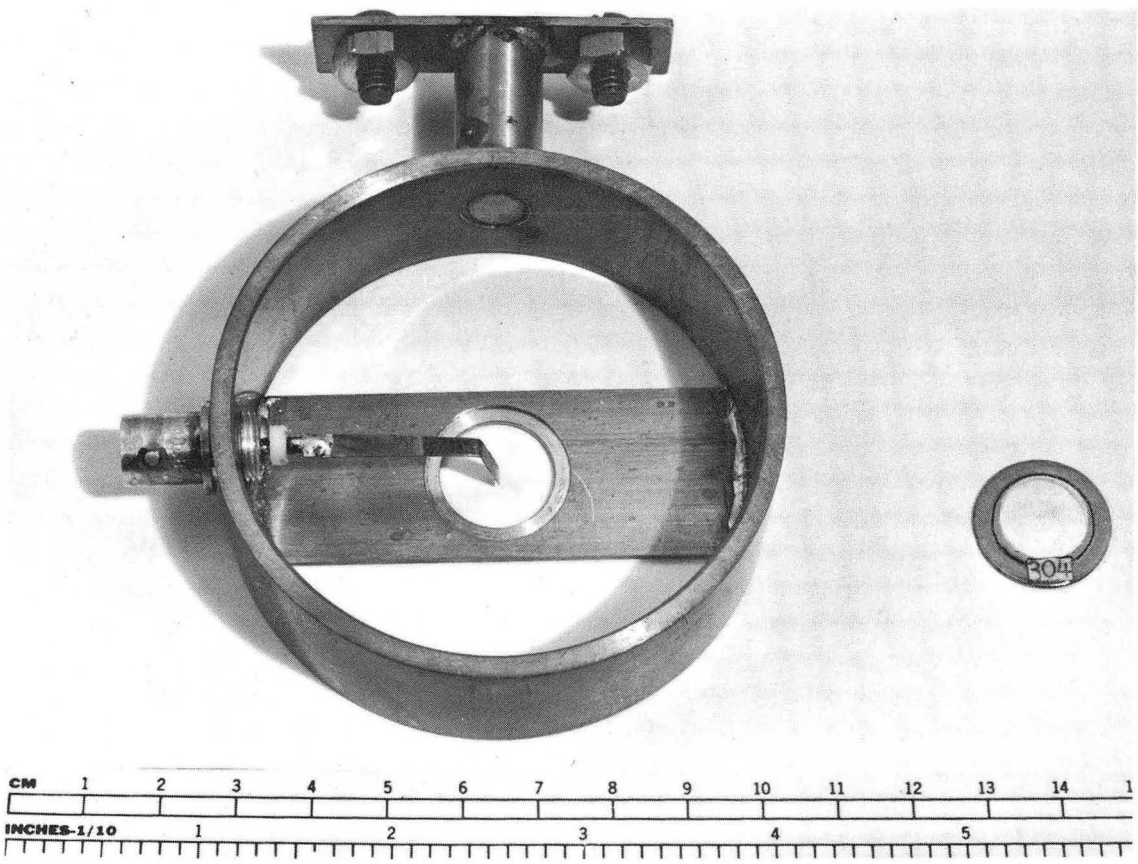

ZN-5364

Fig. 6

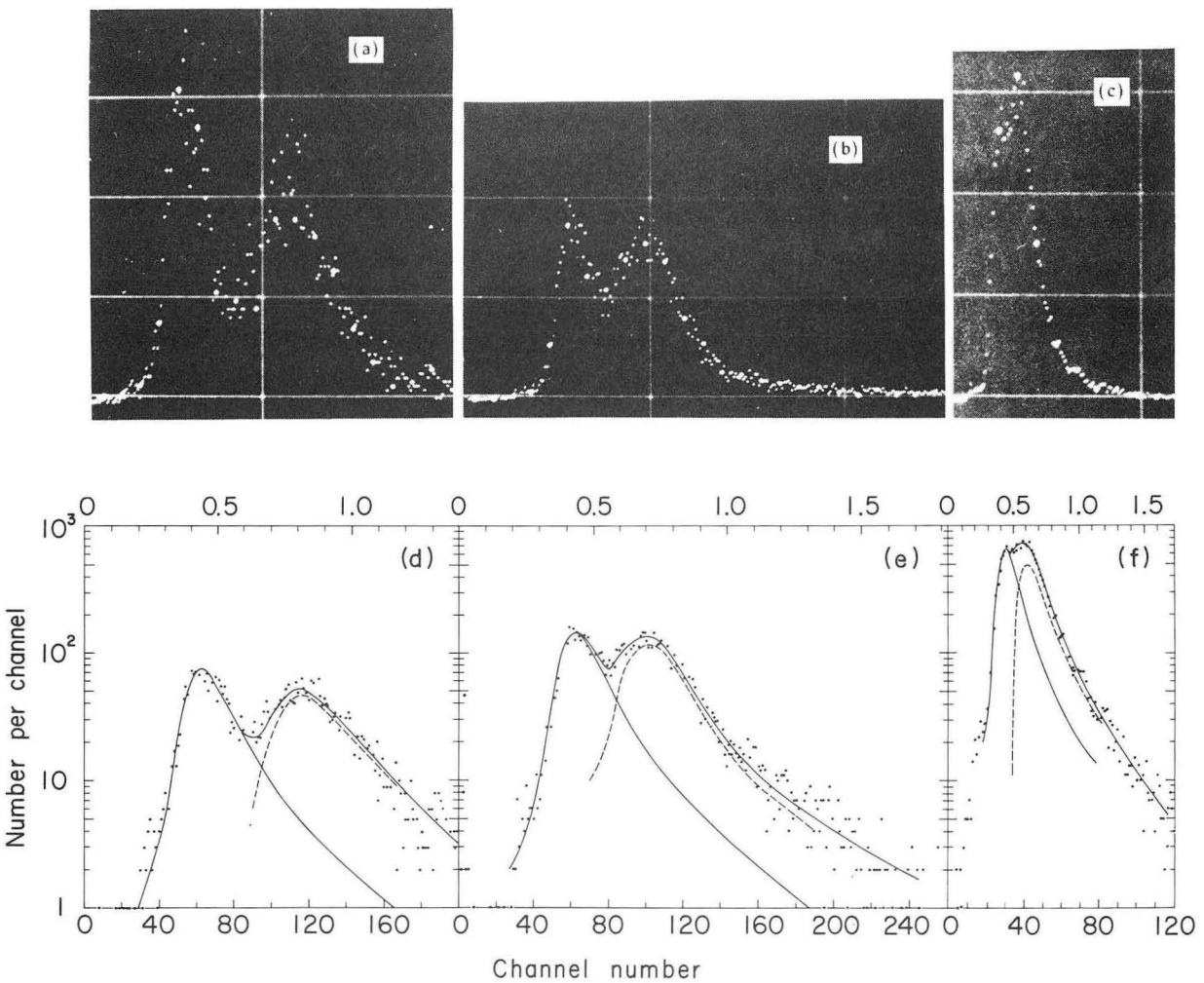

Fig. 7

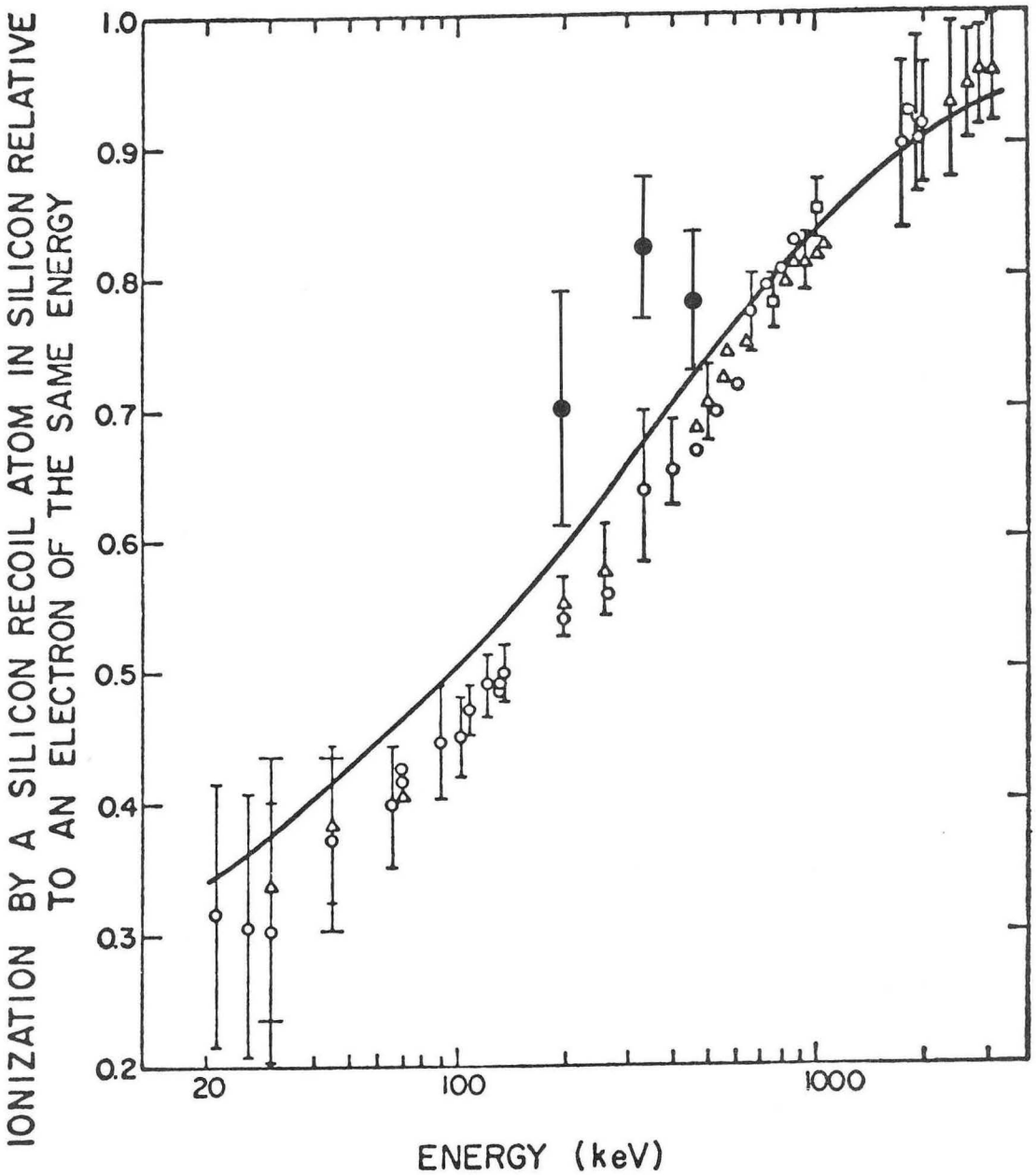

MUB-9234

Fig. 8